Ultrahigh resolution magnetic force microscope tip fabricated using electron beam lithography

Paul B. Fischer, Mark S. Wei, and Stephen Y. Chou
Department of Electrical Engineering, University of Minnesota, Minneapolis, Minnesota 55455

(Received 30 June 1993; accepted 16 July 1993)

A novel magnetic force microscope tip has been proposed and fabricated that consists of a ~ 30 nm thick ferromagnetic film coated on one side of a nonmagnetic pillar which is ~ 150 nm wide and over 1.5 μm long. The pillar was fabricated on the apex of a commercial scanning force microscope tip using high-resolution electron beam lithography. The ferromagnetic film was evaporated on the pillar from an angle so that only the pillar, not the rest of the tip, was coated. The coated ferromagnetic film has a trough shape and a tapered end with a tip radius of ~ 10 nm. The film is single domain because of the nanoscale size and shape anisotropy. Compared to conventional Ni wire tips, the new tips have a much smaller, magnetic cross section at the end of the tip, thus offering better imaging resolution and they have lower stray field, thus making them well suited to measuring soft magnetic materials.

I. INTRODUCTION

Magnetic force microscopy (MFM) has recently gained significant attention as a magnetic imaging technique which is non-destructive and is capable of submicron resolution.[1-4] The MFM tip is one of the most important elements in determining the resolution and sensitivity of a MFM. Previously, sharpened Ni wires[1] and magnetically coated atomic force microscope tips[5] have been used as MFM tips. Such tips suffer from several drawbacks. First, the tips may consist of multiple magnetic domains, and are large in area therefore having a broad distribution of magnetic charge. These all result in poor spatial resolution. Second, the tips have a significant magnetic charge that can alter the magnetic properties of the magnetic material under inspection. To avoid such interference, the tip has to be kept rather far away from the sample surface, hence drastically reducing the MFM's resolution.

We have proposed a novel MFM tip that consists of a long nonmagnetic pillar of nanoscale diameter and a ferromagnetic film that covers only part of the pillar but not the rest of a MFM tip.[6] Such a MFM tip has three important advantages. First, because of the nanoscale size and shape anisotropy, the magnetic tip is single domain. Second, due to the sharpness and small effective magnetic cross section of the tip, it offers higher resolution. Third, due to the small magnetic charge, it is less likely to alter the magnetic properties of the sample. We refer to this tip as the single-domain magnetic spike (SMS) tip. In this article, we present one embodiment of such a tip, its fabrication technology, and evaluate its performance.

II. TIP FABRICATION

The SMS tip fabrication process consists of two main steps (Fig. 1). (1) The nonmagnetic pillar was fabricated by contamination electron beam lithography on top of the pyramid of a commercial scanning force microscope (SFM) tip. (2) Ferromagnetic materials, such as nickel or cobalt, were coated on one side of the pillar. In the first step, SFM cantilevers were first sputter coated with 20 nm of gold to prevent charging during the electron beam contamination lithography and to facilitate subsequent focusing on the apex. The tips were then mounted and inserted into a JEOL-840A scanning electron micrograph (SEM) with a diffusion pump vacuum system and a tungsten filament gun. A contamination pillar was then grown on the apex by exposing the tip in spot mode for a specified length of time. Growth is due to electron beam assisted molecular deposition onto the cantilever surface. The deposited material was not intentionally introduced, but originates primarily from the background of the SEM vacuum chamber and from the sample surface itself. Similar contamination deposits have been shown to be mainly composed of carbon and oxygen.[7]

The growth process was optimized to produce long but narrow pillars with small tip radii. Such pillars would fulfill the requirements for high-resolution MFM tips. The accelerating voltage and beam current were the most influential parameters in the growth process. Figure 2 shows the tip length with respect to exposure time for a beam current of 10 pA and an accelerating potential of 15, 25, and 35 kV. In all three cases, the growth rate becomes relatively constant after an initial transient. The growth rate for 35 kV was found to be the highest (0.1 μm/min after the initial transient).

With lower beam currents there was a dramatic increase in growth rate. Figure 3 shows the resulting tip length with respect to beam current when a 25 kV beam is focused onto the apex for 7 min. The higher growth rate at a lower beam current is possibly due to reduced local heating, in accordance with condensation theory.[8]

The accelerating voltage was found to affect the average pillar tip radius of curvature. The average pillar tie radius of curvature was observed to decrease from 30 to 19 nm as the accelerating voltage increased from 15 to 35 kV (Fig. 4). This is possibly due to the convolution of decreased beam diameter and decreased beam broadening at higher accelerating potentials. According to Monte Carlo simulations, an infinitesimally small 15 kV beam is broadened to a radius of 20 nm after traversing through 50 nm of car-

 0734-211X/93/11(6)/2570/4/$1.00 ©1993 American Vacuum Society

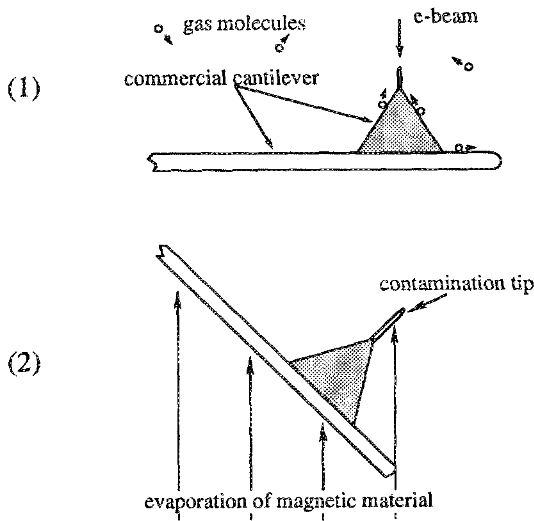

FIG. 1. Schematic of the fabrication process.

bon, while an infinitesimally small 35 kV beam is broadened to only 10 nm after traversing the same amount of carbon.

Based on these pillar growth studies, a beam current of 10 pA, an accelerating potential of 35 kV, and growth times ranging from 7 to 10 min were used to grow the pillars SMS tips. The beam current of 10 pA can maximize the growth rate while maintaining sufficient signal for readily focusing on the tip apex. An accelerating potential of 35 kV was chosen to obtain the smallest tip radius of curvature and obtain the highest growth rates to avoid any system instabilities during the growth. The working distance and magnification for the growth were not found to have a major effect and were maintained at 10 mm and 30 000×, respectively.

After growing the nonmagnetic contamination pillar, the magnetic spike was formed by an evaporation of nickel or cobalt from an angle as illustrated in Fig. 1. The sample is held at an angle with respect to the evaporation source in an electron beam evaporator, so that only the pillar, but not the pyramid, of the tip is coated with ferromagnetic

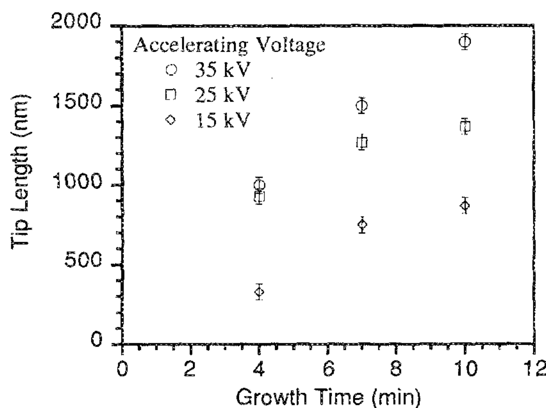

FIG. 2. Tip length with respect to exposure time for a beam current of 10 pA and an accelerating potential of 15, 25, and 35 kV.

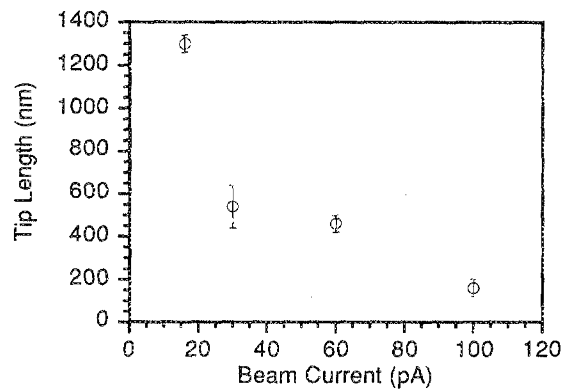

FIG. 3. Characterization of tip length with respect to beam current for a 7 min exposure with a 25 kV beam.

material. In this way, a controllable portion of the tip can be coated with the desired metal. One advantage of this fabrication process is that the thickness of the magnetic material, and thus the effective cross section of the magnetic spike, can be accurately controlled and be kept small. Figure 5 shows a completed MFM tip with a nanoscale nickel magnetic sensor at the tip. The nickel spike, which has a trough shape with a tapered end, is 30 nm thick, 1.4 μm long, and has an average width of ~ 150 nm and a 10 nm tip radius. The nonmagnetic contamination pillar is ~ 1.7 μm long, has an average diameter of ~ 150 nm. The slight bending of the tip is caused by intrinsic tensile stress which is present in evaporated nickel and can be balanced by evaporating nonmagnetic metal on the opposite side of the pillar.

III. TIP ANALYSIS

Calculations were performed to evaluate the performance of the SMS tips. The response of the SMS tip to a magnetic dipole was compared to a standard Ni wire tip (Fig. 6). The full width at half-maximum (FWHM) response for the SMS tip is 40 nm, whereas the FWHM response for a standard Ni wire tip is 60 nm. The calcula-

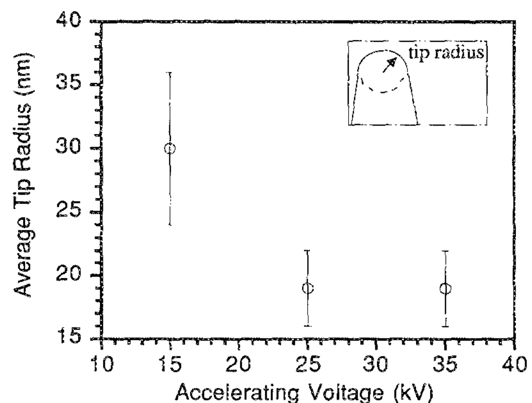

FIG. 4. Characterization of tip radius with respect to accelerating voltage. The insert defines the tip radius. The growth time and beam current were fixed at 10 pA and 7 min, respectively.

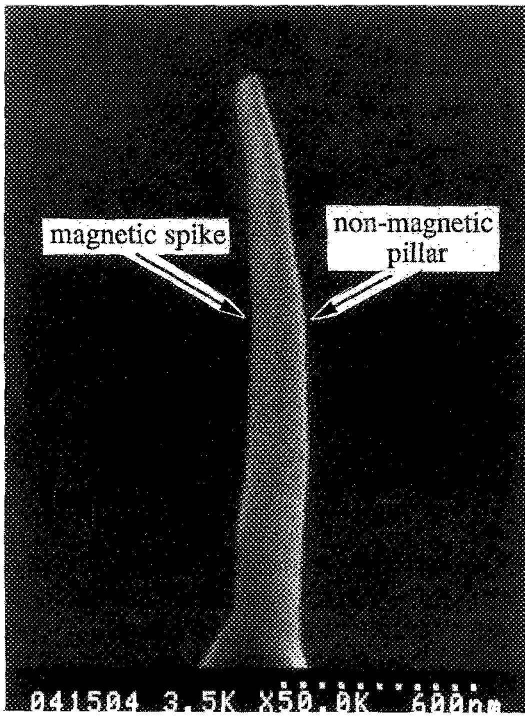

FIG. 5. Completed SMS tip with a nanoscale nickel magnetic sensor at the tip. The Ni spike, which is trough shaped with a tapered end, is 30 nm thick, ~150 nm wide, 1.4 μm long, and has a 10 nm tip radius. The nonmagnetic contamination pillar is ~150 nm wide and 1.7 μm long. Intrinsic stress in evaporated Ni bends the tip.

tion was performed at a tip-to-sample spacing of 50 nm. It also assumes the SMS tip to be rectangular with a thickness of 15 nm, width of 80 nm, and a tip length of 1 μm, and the Ni wire tip to be cylindrical with a radius of 35 nm and a length of 1 μm. In both cases, the magnetization was assumed to be parallel to the tips axis due to shape anisotropy.

The MFM imaging resolution can be further improved by reducing the tip-to-sample spacing. Figure 7 shows the FWHM response of the SMS and Ni wire tips (using the

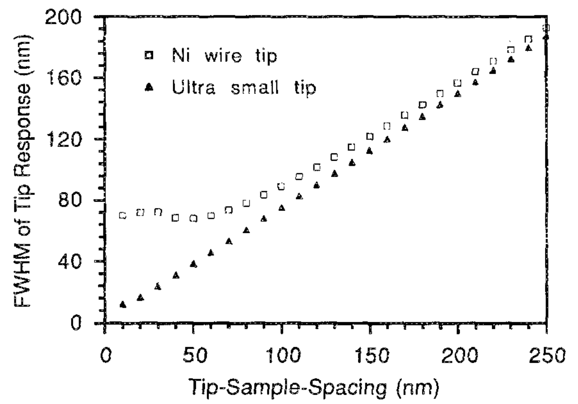

FIG. 7. FWHM response of the SMS and Ni wire tips to a magnetic dipole for different values of tip-to-sample spacing.

same geometry as before) to a magnetic dipole versus the tip-to-sample spacing. For tip-to-sample spacings greater than ~100 nm, the responses of the two tips are similar. At a tip-to-sample spacing of 20 nm, however, the FWHM response of the SMS tip is nearly 20 nm, whereas the Ni wire tip is still ~70 nm. This demonstrates that the ultimate resolution of a MFM tip is limited by its size. The improved resolution of the SMS tip is a direct result of the reduced cross section of the magnetic tip and illustrates the significance of being able to control the size of the magnetic spike.

Another advantage of the SMS tip is a smaller stray field compared to a conventional Ni wire tip (Fig 8). The greatly reduced volume of magnetic material of the SMS tip results in a stray field of only 150 Oe at a distance of 50 nm, making the SMS tip better suited for studying soft magnetic material. Although conventionally coated tips in general also have a stray field smaller than that of a Ni wire tip due to a reduced magnetic volume,[9] the SMS tips offer at least a 50% further reduction.

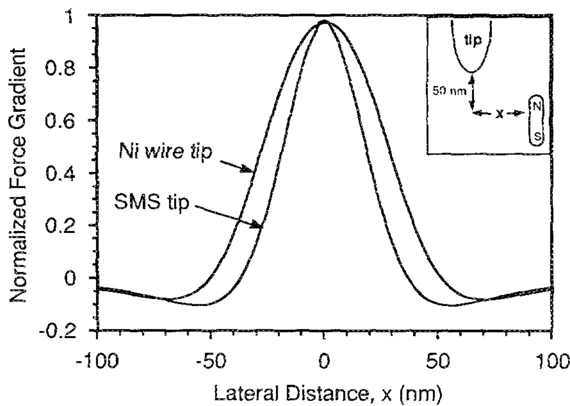

FIG. 6. Response to a magnetic dipole for the SMS tip and a standard Ni wire tip. The FWHM responses are 40 and 60 nm for the SMS and Ni wire tips, respectively.

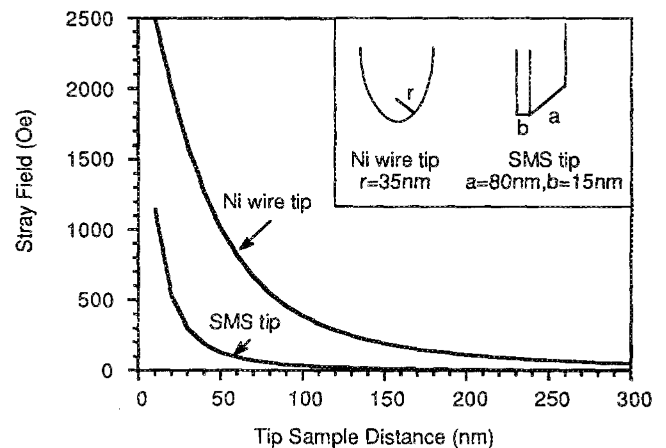

FIG. 8. Stray field of SMS and Ni wire tips.

IV. SUMMARY

We have proposed and fabricated a novel magnetic force microscope tips that consists of a ~30 nm thick ferromagnetic film coated on one side of a nonmagnetic pillar which is ~150 nm wide and over 1.5 μm long. The coated ferromagnetic film has a trough shape and a tapered end with a tip radius of ~10 nm. Such a MFM tip has three important advantages. First, because of the nanoscale size and shape anisotropy, the magnetic tip is single domain. Second, due to the sharpness and small effective magnetic cross section of the tip, it offers higher resolution. Third, due to the small magnetic charge, it is less likely to alter the magnetic properties of the sample. The nonmagnetic pillar was fabricated by contamination electron beam lithography and the ferromagnetic needle was produced using an angle evaporation of nickel or cobalt. Analysis based on a dipole field model indicates that the SMS tip should have a resolution of ~20 nm. Furthermore, the tips should have a stray field less than 150 Oe at a tip to sample spacing of 50 nm, making the tips well suited for measuring soft magnetic material.

ACKNOWLEDGMENTS

The authors are grateful to David Joy for providing Monte Carlo simulation programs. This work was partly supported by the Packard Foundation through a Packard Fellowship to S.C. and the AFOSR through an Air Force Laboratory Graduate Fellowship to P.B.F.

[1] Y. Martin and H. K. Wickramasinghe, Appl. Phys, Lett. **50**, 1455 (1987).
[2] F. Saurenbach and B. D. Terris, Appl. Phys. Lett. **56**, 1703 (1990).
[3] P. Grutter, E. Meyer, H. Heinzelmann, L. Rosenthaler, H.-R. Hidber, and H.-J. Gutherodt, J. Vac. Sci. Technol. A **6**, 279 (1988).
[4] D. Rugar, H. J. Mamin, P. Guethner, S. E. Lambert, J. E. Stern, I. McFadyen, and T. Yogi, J. Appl. Phys. **68**, 1169 (1990).
[5] Y. Honda, S. Hosaka, A. Kikugawa, S. Tanaka, Y. Matsuda, M. Suzuki, and M. Futamoto, Jpn. J. Appl. Phys. **31**, L1061 (1992).
[6] S. Y. Chou (private communication).
[7] Y. Akama, E. Nishimura, A. Sakai, and H. Murakami, J. Vac. Sci. Technol. A **8**, 429 (1990).
[8] A. E. Ennos, Brit. J. Appl. Phys. **4**, 101 (1953).
[9] P. Bryant, S. Schultz, and D. R. Fredkin, J. Appl. Phys. **69**, 5877 (1991).